

The Chemical Application of High-Resolution Electron Tomography: Bright Field or Dark Field?*

John Meurig Thomas,* Paul A. Midgley,*
Timothy J. V. Yates, Jonathan S. Barnard, Robert Raja,
Ilke Arslan, and Matthew Weyland

There are many occasions when chemists need to know detailed information pertaining to the shapes and morphology of minute (nanometer-sized) objects and the topography of nanopores. In characterizing various kinds of electronic devices ranging from quantum dots to quantum wells, in determining the structure of viruses, in visualizing the architecture of supramolecular assemblies inside eukaryotic and prokaryotic cells, and especially in the identification of nanoparticle catalysts supported on high-area nanoporous solids, it is important to know—without recourse to sectioning or other destructive techniques—the precise location, spatial

[*] Prof. Sir J. M. Thomas, Dr. P. A. Midgley, Dr. T. J. V. Yates,
Dr. J. S. Barnard, Dr. I. Arslan
Department of Materials Science and Metallurgy
University of Cambridge
Pembroke Street, Cambridge, CB2 3QZ (UK)
Fax: (+44) 1223-334-563
E-mail: jmt@ri.ac.uk
pam33@cam.ac.uk

Prof. Sir J. M. Thomas
Davy–Faraday Research Laboratory
Royal Institution of Great Britain
21 Albermarle Street, London, W1X 4BS (UK)
Fax: (+44) 207-670-2988

Dr. R. Raja
University Chemical Laboratory, University of Cambridge
Lensfield Road, Cambridge, CB2 1EW (UK)

Dr. M. Weyland
Department of Applied and Engineering Physics
Cornell University, E13 Clark Hall, Ithaca, NY 14853 (USA)

[**] The authors thank the Royal Society, the Isaac Newton Trust, the EPSRC, the IRC in Nanotechnology and the BP and FEI Companies for financial support. We also thank Dr. T. Khimyak and Prof. B. F. G. Johnson for their cooperation.



Supporting information (animation clip) for this article is available on the WWW under <http://www.angewandte.org> or from the author.

distribution, and, wherever possible, the elemental composition of such materials.^[1]

Like other, well-known forms of tomography (X-ray or positron-emission) electron tomography enables a three-dimensional (3D) picture to be computed (by using proven mathematical procedures) from a series of projected two-dimensional (2D) images taken over as wide a range of angular orientations as possible. The greater the number of distinct 2D images accumulated, the higher is the resolution of the resulting tomogram. Typically, the specimens to be investigated are imaged in a high-resolution electron microscope at a series of angular settings (see Figure 1). From such a series, the tomogram (3D picture) is reconstructed by suitable, so-called “back-projection”, as first described by Hart and others.^[2–4]

The question arises, however, as to whether the electron tomographic analysis should be performed under so-called “bright-field” (BF) or “dark-field” conditions. In BF conditions (see Figure 1), in either conventional transmission

nature of the porosity of zeolites and nanoporous silica and the distribution of finely divided noble-metal catalysts within them.^[7–11]

But when attempts are made to extend the resolution of BF electron tomography certain insurmountable, electron-optical drawbacks are encountered. The coherence of the BF signal leads to strong contrast, such as Fresnel contrast, whenever the electron wave encounters a change in refractive index, or diffraction contrast (that produce bend contours and thickness fringes) seen in crystalline specimens. In weakly scattering, noncrystalline samples, these effects are less severe and phase contrast, seen in the image by defocusing, can reveal useful detail. However, phase contrast is highly dependent on the so-called contrast transfer function of the microscope and to reveal very small structures (such as nanoparticles in mesopores, see below) it is necessary to use large defocus values. With large defocus settings, the contrast transfer function oscillates rapidly and direct interpretation of image contrast becomes impossible. For tomography, in which truly 3D samples must be examined, this problem is compounded as identical features at different heights in the specimen can show opposite contrast or no contrast at all. Using small defoci settings will not yield sufficient phase contrast to allow fine detail to be resolved above a support film or substrate, as illustrated later.

High-angle annular dark-field (HAADF) electron tomography, which is readily carried out using a scanning transmission electron microscope (STEM), suffers from none of those drawbacks.^[10,12] Electron beams scattered by the specimen to high angles conform closely to Rutherford's scattering law (where the scattered intensity is proportional to Z^2 , Z = atomic number of the scattering element) and the process is incoherent, so that the signals accumulated by a HAADF detector (Figure 1) are free from the complications arising from the contrast transfer function, adumbrated above. An authentic image of the internal structure of the specimen is thus recorded, and there are no “missing” atomic spacings (as in BF coherent imaging) arising from purely electron-optical effects. A further advantage with STEM imaging is that specimens can suffer far less beam damage during investigation (which is rather long because several images, typically 70, over an angular span of $+70^\circ$ to -70° of specimen tilt, have to be recorded).

Herein we illustrate, with two examples, the veracity of our statement that HAADF electron tomography is superior to BF electron tomography. In the first example, we focus on the bimetallic nanoparticle catalysts, $[\text{Ru}_{10}\text{Pt}_2]$, supported on mesoporous silica. Figure 2a shows images of a typical region of mesoporous silica containing this catalyst under BF conditions; and Figure 2b shows precisely the same region of the specimen recorded under HAADF conditions. Whereas under BF conditions the nanoparticles are barely visible, because of the extremely weak phase contrast, under HAADF conditions they stand out clearly because of the high amplitude, atomic number contrast.^[13]

Figure 3 shows a series of 3 nm thick slices of the tomogram (derived from images such as that shown in Figure 2b) displayed parallel to the pore axis at intervals of 5 nm—an animation of the top-to-bottom distribution of

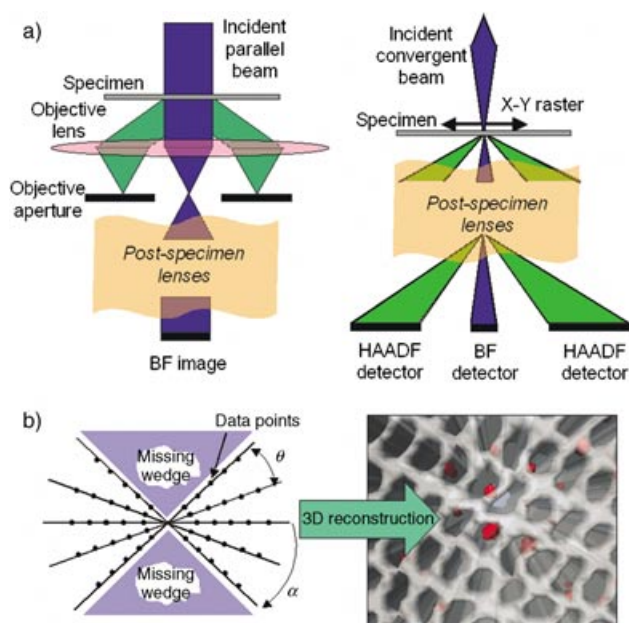


Figure 1. a) Bright field (BF) image formation in the TEM (left) and BF and high-angle annular dark-field (HAADF) image formation in the STEM (right). b) Fourier space representation (left) of the series of images, angular sampling θ , maximum tilt α , used to reconstruct a tomogram, such as that of the mesoporous catalyst (right).

(TEM) or scanning transmission (STEM) mode, the forward-scattered beam is used to construct the electron microscopic images (2D) images, whereas in the dark field conditions, it is the beams diffracted through high angles that form the images. BF imaging is the customary procedure, especially in molecular biological contexts; for example in the cryo-electron microscopic, tomographic work of Baumeister et al. a great deal of insight has been gained in visualizing the molecular organization of the cytoplasm using BF-based tomography.^[5,6] It has also been used effectively to clarify the

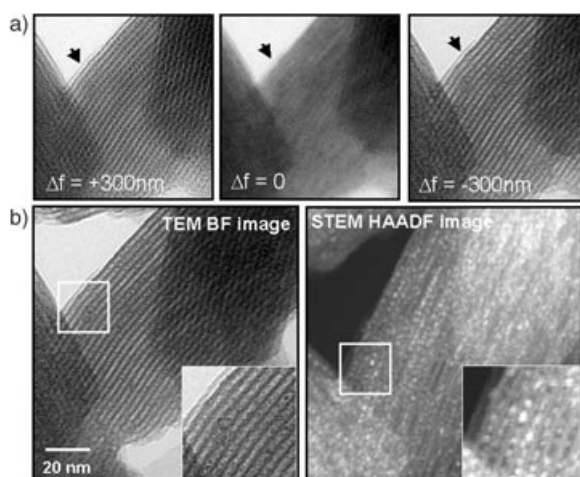


Figure 2. a) BF images, taken at three defocus values, of nanoparticle-filled mesoporous silica. b) A comparison of BF (left) and HAADF (right) images of identical areas of catalyst: nanoparticles of $[\text{Ru}_{10}\text{Pt}_2]$ invisible in BF are clearly seen in the HAADF image.

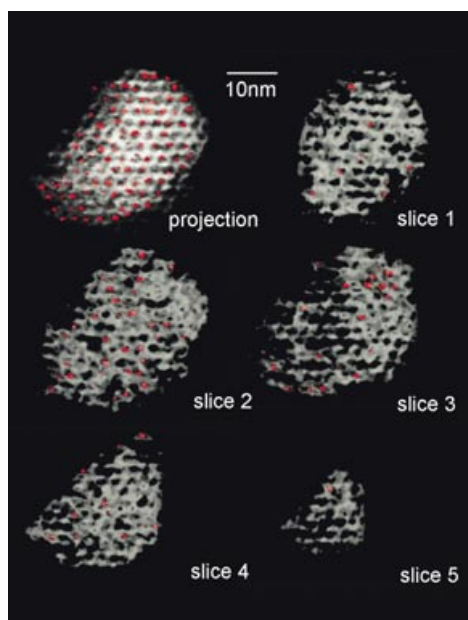


Figure 3. An axial projection of a 30 nm thick specimen and five successive 3-nm thick slices through a tomogram of silica-supported $[\text{Ru}_{10}\text{Pt}_2]$: nanoparticles (red), mesoporous silica (white).

$[\text{Ru}_{10}\text{Pt}_2]$ nanoparticles within the mesoporous silica is in the Supporting Information.

In the second example, we take a section of a Si-Ge multiple quantum-well device, recorded both under BF (Figure 4a) and HAADF (Figure 4b) conditions. Again, the benefits of dark-field imaging are clear. The BF image is dominated by coherent diffraction contrast (bend contours) and the quantum wells are barely visible. In the HAADF micrograph the diffraction contrast has disappeared and the image is dominated by thickness and atomic number contrast—the wells contain 15% Ge. Such an image contrast is ideal for subsequent tomographic analysis.

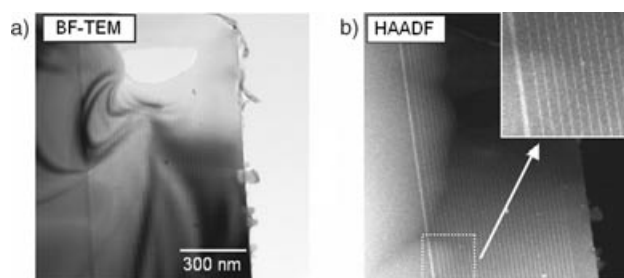


Figure 4. a) TEM BF image and b) STEM HAADF image of a Si-Ge multiple quantum well structure. Coherent diffraction effects dominate the BF image. The quantum wells are revealed clearly only in the incoherent HAADF image.

The quintessential conclusion to be drawn from this work is that when electron tomographic resolutions of 3 to 6 nm are deemed adequate, BF imaging suffices. At higher resolutions, and especially in probing nanoparticles of dimension 1 nm or less, it is imperative that HAADF tomography be employed.

Received: July 27, 2004

Published online: November 26, 2004

Keywords: electron tomography · heterogeneous catalysis · nanoparticles · scanning probe microscopy

- [1] J. M. Thomas, P. A. Midgley, *Chem. Commun.* **2004**, 1247.
- [2] R. G. Hart, *Science* **1968**, 159, 1464.
- [3] D. J. De Rosier, A. Klug, *Nature* **1968**, 217, 130.
- [4] R. A. Crowther, L. A. Amos, J. T. Finch, A. Klug, *Nature* **1970**, 226, 421.
- [5] O. Medalia, I. Weber, A. S. Frangakis, G. Gerisch, W. Baumeister, *Science* **2002**, 298, 1209.
- [6] J. M. Plitzko, A. S. Frangakis, S. Nickell, F. Forster, A. Gross, W. Baumeister, *Trends Biotechnol.* **2002**, 8, S41.
- [7] A. H. Janssen, A. J. Koster, K. P. de Jong, *J. Phys. Chem. B* **2002**, 106, 11905.
- [8] K. P. de Jong, A. J. Koster, *ChemPhysChem* **2002**, 3, 776.
- [9] U. Ziese, K. P. de Jong, A. J. Koster, *Appl. Catal. A* **2004**, 260, 71–74.
- [10] P. A. Midgley, M. Weyland, J. M. Thomas, B. F. G. Johnson, *Chem. Commun.* **2001**, 18, 907.
- [11] P. A. Midgley, J. M. Thomas, L. Laffont, M. Weyland, R. Raja, B. F. G. Johnson, T. Khimyak, *J. Phys. Chem. B* **2004**, 108, 4590.
- [12] P. A. Midgley, M. Weyland, *Ultramicroscopy* **2003**, 96, 413.
- [13] The apparent size of the nanoparticles depends on the precise imaging conditions (e.g. a larger probe size results in a “larger” particle). In reality the $[\text{Ru}_{10}\text{Pt}_2]$ particles are approximately 0.4 nm diameter.